FATIGUE BEHAVIOUR OF SURFACE-CRACKED SHELLS

Andrea Carpinteri, Roberto Brighenti, Andrea Spagnoli

Dipartimento di Ingegneria Civile, Università di Parma,
Parco Area delle Scienze 181/A, 43100 Parma, ITALY
E-mail: carpint@parma1.eng.unipr.it

Abstract

A portion of a flawed thin-walled shell with an elliptical-arc external surface flaw located in a straight zone (pipe) or in a joint zone (elbow) is analysed to evaluate stress field and fatigue life. Such a portion is assumed to be a part of a shell of revolution, described by two principal curvature radii (R_1 and R_2). By employing the superposition principle and the power series expansion of the actual stresses, an approximated stress-intensity factor (SIF) expression can be determined for different actual loading conditions. In the present paper, the SIFs (weight functions) for five elementary stress distributions are determined through a FE analysis, by varying the relative curvature radius $r = R_1 / R_2$ of the shell from 0 to ∞. Then, the SIFs for cylindrical and spherical shells under various loading conditions are computed through the above weight functions. Finally, a numerical simulation is carried out to predict the crack growth under cyclic internal pressure with constant amplitude. Some results are compared with those determined by other authors.

Sommario

La valutazione del campo tensionale e del comportamento a fatica di gusci fessurati viene condotta considerandone una porzione nell'intorno della zona danneggiata; tale porzione di guscio può avere singola o doppia curvatura ed è ipotizzata come parte di un guscio di rivoluzione avente due raggi principali di curvatura, R_1 ed R_2. Utilizzando il principio di sovrapposizione e sviluppando in serie di potenze la reale distribuzione di sforzi agente, è possibile determinare in modo approssimato il corrispondente valore dello SIF. Nella presente nota, i valori degli stress-intensity factors (SIF), o funzioni peso, per cinque distribuzioni elementari di tensione sono ottenuti mediante un' analisi agli elementi finiti, variando il raggio relativo di curvatura ($r = R_1 / R_2$) del guscio da 0 ad ¥. Mediante le suddette funzioni peso vengono poi ricavati i valori dei SIF per gusci cilindrici e sferici soggetti a varie condizioni di carico. Infine, tramite una simulazione numerica, viene determinato l'accrescimento a fatica della fessura superficiale nel caso di pressione interna

ciclica ad ampiezza costante. Alcuni risultati sono confrontati con valori reperibili in letteratura.

1. Introduction

Structural safety of pressure vessels, such as pipes, elbows, end closures, domes, should be assessed also by taking into account the influence of flaws, inclusions, cracks and so on. As a matter of fact, these defects can remarkably affect the reliability of such components, especially when they are subjected to time-varying loading. Several analyses of cracked pipes under tension and bending [1-4] or internal pressure [5-8] have been carried out, but only a few authors [9-11] have examined part-through-cracked double-curvature shells, due to the complexity of such flawed configurations.

In the present paper, a portion of a thin-walled shell is considered as a part of a toroidal shell having the wall thickness t comparatively small in comparison with the principal curvature radii, R_1 and R_2 (Fig.1). An external part-through defect is assumed to initiate due to damage and then propagate under cyclic loading. For sake of semplicity, the external surface flaw is assumed to lie in one of the principal curvature planes (Fig.1), and to present an elliptical-arc shape with aspect ratio $\alpha = a/b$ and relative depth $\chi = a/t$ of the deepest point A on the defect front, where a is the maximum crack depth. The fatigue fracture analysis of the above cracked shell is in accordance with some recommendations [12,13] which suggest to replace an actual surface defect by an equivalent elliptical-arc flaw.

Firstly the stress-intensity factors (SIFs) along the crack front for five elementary opening stress distributions (constant, linear, quadratic, cubic and quartic) acting on the crack faces are determined by performing a three-dimensional finite element analysis. Then approximate SIFs in cylindrical, toroidal and spherical shells under internal pressure, membrane stresses and local bending are computed through the above elementary SIFs, by exploiting the superposition principle and the power series expansion of the actual stresses. Finally, a numerical simulation is carried out to predict the crack growth in shells under cyclic internal pressure. Comparisons between the present results and those deduced by other authors are shown.

2. Geometrical parameters

The two principal curvature radii of the shell of revolution in Fig.1 are called R_1, in the flaw plane, and R_2, in a plane perpendicular to the flaw plane, respectively. The relative curvature radius r^* of the shell at the crack location is defined by the ratio between the above radii, i.e. $r^* = R_1 / R_2$. In the following, the defect is termed transversal-like for $R_1 < R_2$ (i.e. $r^* < 1$) and longitudinal-like for $R_1 > R_2$ (i.e. $r^* > 1$). The case of $R_1 = R_2$ refers to a portion of a spherical shell, for which it is meaningless to distinguish between a transversal flaw and a longitudinal flaw. Seven different cracked shell geometries are examined: $r^* = 0$ (cylindrical shell with a transversal flaw), $r^* = 1/10,\ 1/3$ (toroidal shells with a transversal-like flaw), $r^* = 1$ (flawed spherical shell), $r^* = 3,\ 10$ (toroidal shells with a longitudinal-like flaw) and $r^* = \infty$ (cylindrical shell with a longitudinal flaw).

The dimensionless wall thickness of the shell is defined as $R^* = R_1 / t$ for $r^* < 1$ and $R^* = R_2 / t$ for $r^* > 1$; for a spherical shell, $R^* = R_1 / t = R_2 / t$. In the following, R^* is

assumed to be constant and equal to 10.

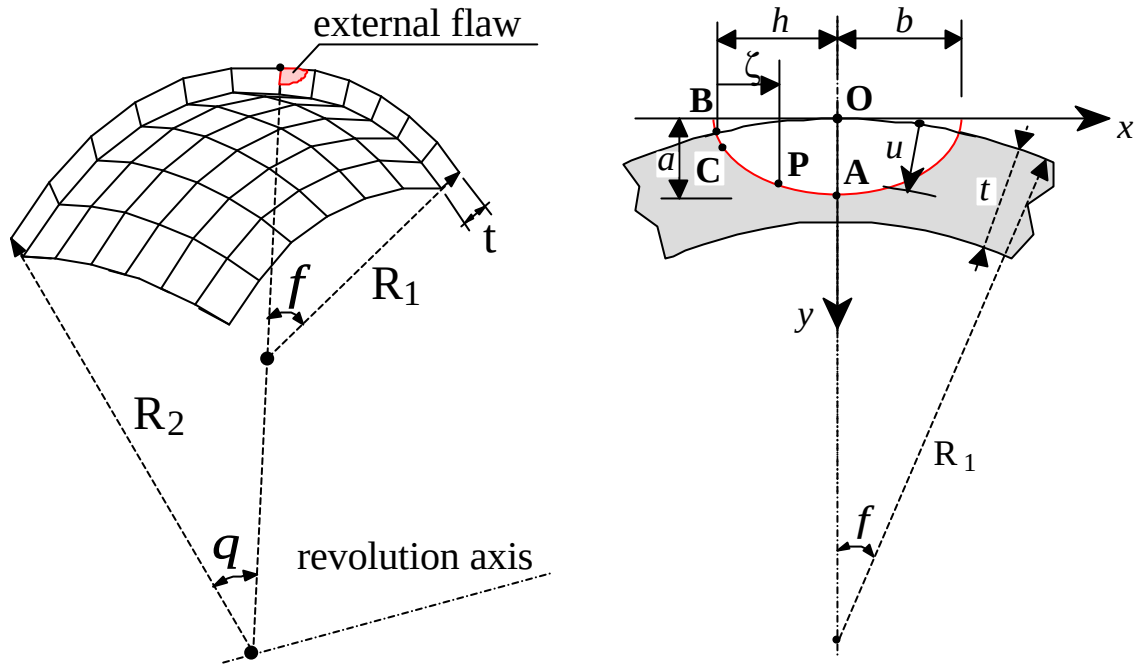

Figure 1
Doubled-curvature cracked shell

3. Approximate stress-intensity factors

The SIF of a cracked body under a given stress field is equal to the SIF produced by the stress distribution, acting on the faces of the crack and having the same magnitude but opposite sign with respect to the corresponding distribution in the body without cracks. Five elementary opening stress distributions acting on the crack faces are considered:

$$\sigma_{I(n)} = (u/a)^n = \eta^n \qquad n = 0,...,4 \tag{1}$$

where $\eta = u/a$ is a dimensionless radial coordinate, with origin on the external surface of the shell (Fig. 1). For the n-th elementary opening stress distribution, the dimensionless Mode I stress-intensity factor, which can be regarded as an influence function or a weight function, is given by:

$$K^*_{I(n)} = K_{I(n)} / \left(\sigma_{ref(n)} \sqrt{\pi a}\right) \tag{2}$$

where $\sigma_{ref(n)} = 1$ and $K_{I(n)}$, the SIF related to the n-th load case, is obtained from the displacements determined through a three-dimensional finite element analysis.

An approximate expression of a complex opening stress distribution, $\sigma_{I(L)}(u)$, where the subscript (L) indicates the generic load case, can be deduced by employing a truncated power series expansion of the actual opening stress and the superposition principle. The corresponding dimensionless SIF can be expressed as follows :

$$K^*_{I(L)} \cong \frac{1}{\sigma_{ref(L)}} \sum_{n=0}^{4} B_{n(L)} \; K^*_{I(n)} \text{ ; whith } B_{n(L)} = a^n \left[\frac{1}{n!} \frac{d^{(n)}}{du^{(n)}} \left(\sigma_{I(L)}(u) \right) \right] \qquad (3)$$

Common stress conditions for shells can be described through membrane stresses, corresponding to a constant stress distribution on the crack faces, or local bending stresses, corresponding to a linear combination of constant and linear stress distributions on the crack faces. In the case of a local bending, the linear stress distribution can be obtained from the following expression:

$$\sigma_{I(b)}(u) = \overline{\sigma_{I(b)}} \left(\sigma_{I(0)} - 2 \chi \sigma_{I(1)} \right) \qquad (4)$$

where $\overline{\sigma_{I(b)}}$ is the maximum value of the actual bending opening stress. Analogously, the dimensionless SIF for a local bending can be deduced as follows:

$$K^*_{I(b,t)} = K^*_{I(0)} - 2 \chi K^*_{I(1)} \qquad (5)$$

where the subscripts *b* and *t* stand for bending and toroid, respectively.

4. SIF results

The dimensionless SIFs, $K^*_{I(n)}$, for the elementary opening stresses given in Eqn (1) are determined through Eqn (2) and a 3-D finite element analysis. As an example, Figure 2 shows $K^*_{I(0)}$ (constant stress distribution) against ζ^*, in the case of $\chi = 0.3$ and the relative curvature radius $r^* = R_1 / R_2$ equal to 1/10, 1 (spherical shell) and 10, respectively. The parameter $\zeta^* = \zeta / h$ defines the position of the generic point *P* along the crack front (Fig. 1). The maximum SIF along the crack front is attained at the deepest point *A* ($\zeta^* = 1.0$) for low values of α, and at point *C* ($\zeta^* = 0.1$) for high values of α.

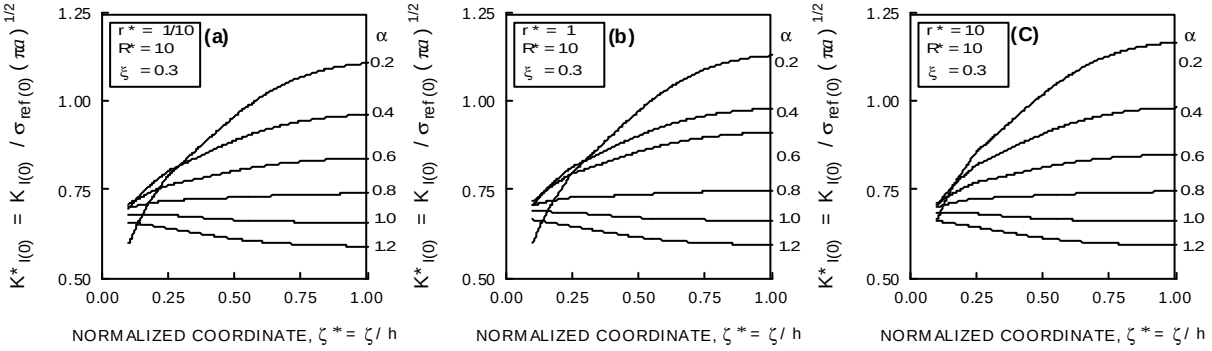

Figure 2
Dimensionless SIF under membrane loading for $\chi = 0.3$ and different values of α: (a) shell with a transversal-like flaw; (b) spherical shell; (c) shell with a longitudinal-like flaw

Some of the SIF results determined for membrane and bending loading are reported in Table

1 in the case of $r^* = 0$, 1/3, 3 and ∞, for $\chi = a/t$ = 0.1, 0.5, 0.8, and $\alpha = a/b$ = 0.2, 0.6, 1.0. Furthermore, the dimensionless SIF K'_I ($K'_I = K^*_I \sqrt{\chi}$) at the deepest point A against the relative crack depth is plotted for a toroidal shell ($r^* = 1/3$) under membrane loading (Fig. 3(a)) and local bending (Fig. 3(b)). The reference stresses for such loading conditions are $\sigma_{ref(m)} = 1$ and $\sigma_{ref(b)} = \overline{\sigma_{I(b)}}$, respectively. Each curve refers to a flaw with a constant value of the ratio b/t (equal to 0.5, 1.0, 2.0, 4.0) and, consequently, the crack aspect ratio α changes along a given curve.

Table 1
Dimensionless SIF for cracked shell under membrane and bending loading

		r* = 0						**r* = 1/3**					
		(a) $K^*_{I(0)}$			**(b)** $K^*_{I(b)}$			**(a)** $K^*_{I(0)}$			**(b)** $K^*_{I(b)}$		
α	**χ**	**0.1**	**0.5**	**0.8**	**0.1**	**0.5**	**0.8**	**0.1**	**0.5**	**0.8**	**0.1**	**0.5**	**0.8**
0.2	**A**	0.9083	1.3519	1.6168	0.7923	0.6134	0.2725	0.8961	1.3823	1.6913	0.7817	0.6318	0.3097
	C	0.5373	0.7153	0.9663	0.5099	0.5671	0.6252	0.5288	0.7214	0.9738	0.5018	0.5719	0.6287
0.6	**A**	0.7511	0.9201	0.9949	0.6498	0.3481	0.0154	0.7381	0.9338	1.0133	0.6385	0.3558	0.0264
	C	0.6317	0.8002	0.9610	0.5882	0.5416	0.4880	0.6249	0.8093	0.9802	0.5819	0.5476	0.4972
1.0	**A**	0.6105	0.6907	0.7161	0.5224	0.3275	*-0.0743*	0.5990	0.6980	0.7209	0.5125	0.2202	*-0.0701*
	C	0.6288	0.7263	0.8011	0.5826	0.4669	0.3571	0.6235	0.7325	0.8115	0.5776	0.4709	0.3622

		r* = 3						**r* = ¥**					
		(a) $K^*_{I(0)}$			**(b)** $K^*_{I(b)}$			**(a)** $K^*_{I(0)}$			**(b)** $K^*_{I(b)}$		
α	**χ**	**0.1**	**0.5**	**0.8**	**0.1**	**0.5**	**0.8**	**0.1**	**0.5**	**0.8**	**0.1**	**0.5**	**0.8**
0.2	**A**	0.9026	1.5414	2.1719	0.7876	0.7289	0.5137	0.8730	1.5400	2.2781	0.7608	0.7251	0.5379
	C	0.5433	0.8155	1.2026	0.5120	0.6085	0.7127	0.5425	0.8310	1.2616	0.5090	0.5729	0.6371
0.6	**A**	0.7422	0.9559	1.0565	0.6422	0.3689	0.0424	0.7158	0.9231	1.0325	0.6182	0.3490	0.0267
	C	0.6273	0.8189	1.0122	0.5836	0.5416	0.4823	0.6060	0.7758	0.9470	0.5635	0.5061	0.4321
1.0	**A**	0.6015	0.7050	0.7310	0.5148	0.2243	*-0.0664*	0.5822	0.6783	0.7172	0.4973	0.2087	-0.0751
	C	0.6263	0.7386	0.8267	0.5801	0.4707	0.3587	0.6011	0.6988	0.7817	0.5566	0.4420	0.3303

The agreement between the present results and those by Joseph et al. [10] is quite satisfactory. Negative values of the SIF for very deep flaws in shells under bending appears to be meaningless, since the crack closure leads to zero SIF values. However, such results can be useful in practical cases when the superposition principle is applied.

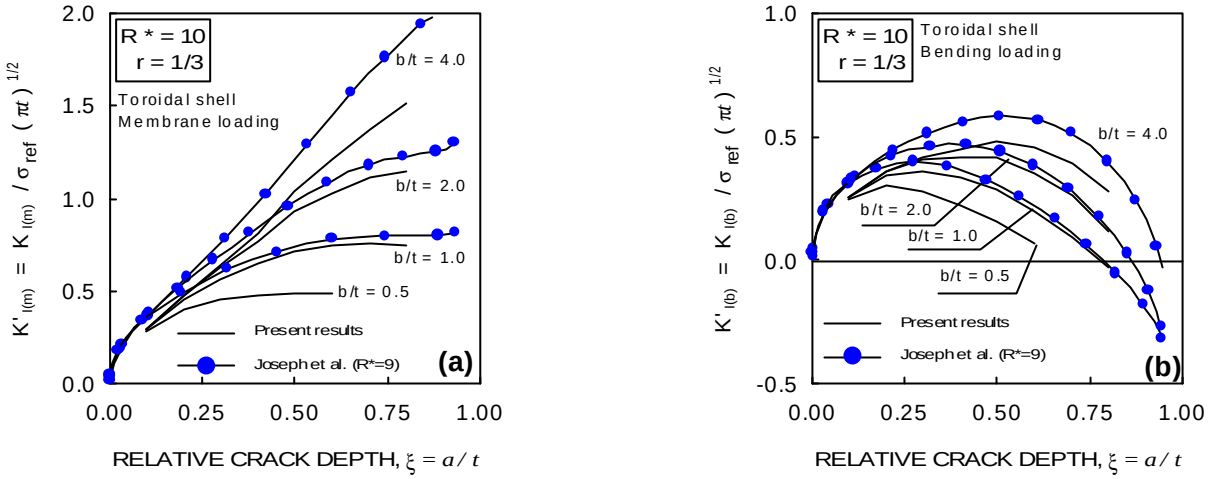

Figure 3
Dimensionless SIF for different values of b/t: (a) membrane loading; (b) bending loading

5. Crack growth under cyclic internal pressure

A cylindrical shell ($r^* = \infty$) and a spherical shell ($r^* = 1$) under cyclic internal pressure with a constant amplitude are examined by employing a two-parameter theoretical model [14] based on the Paris-Erdogan law ($da/dN = \mathrm{Q}\,(\Delta K_I)^m$), where Q and m have been assumed equal to 1.83×10^{-13} and 3 respectively, with da/dN in mm cycle^{-1} and the SIF range ΔK_I in N mm$^{-3/2}$. Some results are shown in the diagram of α against χ in Fig. 4(a), for seven initial crack configurations. Results by Lin et al. [6] for a cylindrical shell are also reported. It can be observed that the flaws considered tend to follow preferred propagation paths for both a cylindrical and a spherical shell, with slightly lower values of α in the latter case. The interpolants of two curves for $r^* = 1$ (in the range $0.2 \le \chi \le 0.8$) are given by :

point 1: $(\chi_0, \alpha_0) = (0.2; 0.2)$, i.e. an initial nearly straight-fronted flaw

$$\alpha = -0.0692 + 1.4076\,\chi - 0.2964\,\chi^2 - 0.3375\,\chi^3$$

point 5: $(\chi_0, \alpha_0) = (0.2; 1.0)$, i.e. an initial circular-arc-fronted flaw

$$\alpha = 1.0575 - 0.4510\,\chi + 0.7997\,\chi^2 - 0.5550\,\chi^3 \qquad (6)$$

The crack depth evolution with the loading cycles is displayed in Fig. 4(b) for the flaws No.1 and No.5 analysed in Fig. 4(a). As can be observed, for a given value of r^*, the surface crack grows more rapidly for a low initial aspect ratio α_0. Furthermore, for a fixed flaw (χ_0, α_0), the number of loading cycles to attain a given value of χ is much greater in the case of a spherical shell ($r^* = 1$) than in the case of a cylindrical shell ($r^* = \infty$).

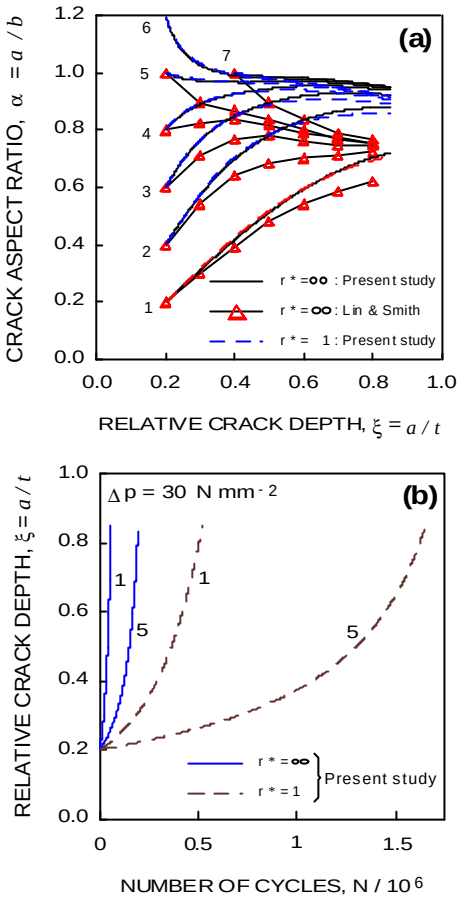

Figure 4
(a) crack patterns; (b) $\boldsymbol{x} - N$ *curves for the cracked shells examined*

6. Conclusions

An elliptical-arc external flaw in a double-curvature thin-walled shell has been examined. The stress-intensity factor (SIF) distributions under different opening stresses acting on the crack faces have been determined through a 3-D finite element analysis for several values of the relative curvature radius $r^* = R_1 / R_2$, where R_1 and R_2 are the principal curvature radii of the toroidal shell considered. Longitudinal-like flaws ($r^* > 1$) show greater values of SIF with respect to transversal-like flaws ($r^* < 1$) under the same type of loading, especially for low values of $\boldsymbol{a}$ and high values of $\boldsymbol{x}$. Then the SIFs for toroidal shells under membrane loading, local bending and internal pressure have been deduced by employing the superposition principle and the power series expansion concept. Finally, the fatigue crack growth under cyclic internal pressure has been examined in the case of a cylindrical and a spherical shell. The agreement between the present results and those determined by other authors is quite satisfactory.

Acknowledgements

The authors gratefully acknowledge the research support for this work provided by the Italian Ministry for University and Technological and Scientific Research (MURST) and the Italian National Research Council (CNR).

References

[1] Raju I.S., Newman J.C., *"Stress intensity factors for circumferential surface cracks in pipes and rods"*, In: "Fracture Mechanics: Seventeenth Volume", ASTM STP 905, 789-805, **1986**.

[2] Bergman, M., *"Stress intensity factors for circumferential surface cracks in pipes"*, Fatigue Fracture Engng Mater. Struct., **18**, 1155-1172, **1995**.

[3] Carpinteri A., Brighenti R., Spagnoli A., *"Part-through cracks in pipes under cyclic bending"*, Nuclear Engng Design, **185**, 1-10, **1998**.

[4] Carpinteri A., Brighenti R., *"Circumferential surface flaws in pipes under cyclic axial loading"*, Engng Fract. Mech., **60**, 383-396, **1998**.

[5] Nishioka T., Atluri S.N., *"Analysis of surface flaw in pressure vessel by new 3-dimensional alternating method*", J. Pressure Vessel Tech., **104**, 299-307, **1982**.

[6] Lin X.B., Smith R.A., *"Numerical analysis of fatigue growth of external surface cracks in pressurised cylinders*", Int. J. Pressure Vessels Piping, **71**, 293-300, **1997**.

[7] Raju I.S., Newman J.C. Jr, *"Stress-intensity factors for internal and external surface cracks in cylindrical vessels*", J. Pressure Vessel Tech., **104**, 293-298, **1982**.

[8] Carpinteri A., Brighenti R., Spagnoli A., *"Fatigue growth of axial surface cracks in hollow cylinders"*, Proc. of the 8th Int. Conf. on Mech. Behaviour of Materials (ICM 8), 183-188, Victoria (British Columbia), Canada, **1999**.

[9] Joseph P.F., Erdogan F., *"A surface crack in shells under mixed-mode loading conditions*", J. of Applied Mech., **55**, 795-804, **1988**.

[10] Joseph P.F., Cordes R. D., Erdogan F., "*Surface cracks in toroidal shells*", Nuclear Engng. and Design, **158**, 263-276, **1995**.

[11] Mohan R., *"Fracture analyses of surface-cracked pipes and elbows using the line-spring/shell model*", Engng. Fract. Mech., **59**, 425-438, **1998**.

[12] ASME Boiler and Pressure Vessel Code, Section XI. *"Rules for inservice inspection of nuclear power plant components"*, American Soc. Mechanical Engineers, U.S.A., **1981**.

[13] *Guidance on some methods for the derivation of acceptance levels for defects in fusion welded joints, Section 3*, British Standards Institution, BSI PD6493, **1991**.

[14] Carpinteri A. (Editor), *"Handbook of Fatigue Crack Propagation in Metallic Structures"*, Elsevier Science Publishers B.V., Amsterdam, The Netherlands, **1994**.